INFACON 7, Trondheim, Norway, June 1995
Eds.: Tuset, Tveit and Page
Publishers: FFF, Trondheim, Norway

THERMODYNAMICS OF PHOSPHORUS IN CARBON-SATURATED MANGANESE-BASED ALLOYS

S.C.Shim and N.Sano
Department of Metallurgy, The University of Tokyo, Tokyo, JAPAN

ABSTRACT

Removal of phosphorus from manganese-based alloys is difficult due to the preferential oxidation of manganese. Recently we have found that the BaO-MnO flux system is efficient for this purpose. Accordingly, the present study has been performed to provide thermodynamic data for manganese-based alloys. A slight decrease in the activity coefficient of phosphorus in Fe-Mn-$C_{satd.}$ alloys was observed with increasing manganese content, reflecting a stronger interaction between manganese and phosphorus than that between iron and phosphorus. We also found that activity of phosphorus in Mn-Si-$C_{satd.}$ alloys significantly increases with increasing silicon content.

INTRODUCTION

Phosphorus is known to be one of the impurities which should be removed from ferro-manganese for the production of non-magnetic Fe-Mn alloys. However, its removal by the conventional dephosphorization method by oxidation is difficult due to the preferential oxidation of manganese. Recently we have found that the BaO-MnO system is efficient to serve this purpose as shown in FIG.1.[1)] Accordingly, a series of works have been undertaken in our group to know the thermodynamic properties of phosphorus in Fe-Mn alloys in order that their contribution with the information on the phosphorus distribution ratio between the flux and metals may contribute to understanding the whole picture of phosphorus behavior in the flux treatment. Since the details of the present study will be published later, the summary of what has been known up to now will be described in this presentation with emphasis on discussion.

I. DETERMINATION OF THE ACTIVITY COEFFICIENT OF PHOSPHORUS IN CARBON SATURATED Fe-Mn ALLOYS

The phosphorus distribution ratios between carbon saturated Fe-Mn alloys and the $BaO-BaF_2$ system in a graphite crucible, $L_P(Fe\text{-}Mn\text{-}C_{satd.})$ were measured at 1573 K in an Ar-CO mixture having the oxygen partial pressure of 3.38×10^{-18} atm(P_{CO}=0.333atm) at 1573K and 7.89×10^{-17} atm(P_{CO}=1atm) at 1673K. Since the $BaO-BaF_2$ system containing 15.0 to 20.2 mass pct of BaO has a very limited solubility of MnO, as shown in FIG.2, the presence of a small amount of MnO was assumed not to affect the activity coefficient of phosphorus in the flux.

The phosphorus distribution for carbon saturated iron without manganese, L_P ($Fe\text{-}C_{satd.}$), had been measured under the same conditions with the same flux, so that Eq.(1) holds.

$$\log \frac{L_P(Fe - Mn - C_{satd.})}{L_P(Fe - C_{satd.})} = \log \frac{f_P(Fe - Mn - C_{satd.})}{f_P(Fe - C_{satd.})} = e^{Mn}_{P,C_{satd}}[\text{mass pct}Mn] \quad (1)$$

where $e_P{}^{Mn}{}_{,C_{satd.}}$ is an interaction parameter between Mn and P at carbon saturation which is not equal to that defined for an infinitely dilute solution of molten iron, and f_P is the activity coefficient of phosphorus in metallic melts. The values for f_P (Fe-$C_{satd.}$) are known as Eq.(2), so that f_P (Fe-Mn-$C_{satd.}$) can be calculated according to Eq.(1), $e_P{}^{Mn}{}_{,C_{satd.}}$ being also estimated.

$$\log f_P(Fe - C_{satd.}) = -\frac{386}{T} + 0.891 \quad ^{2)} \quad (2)$$

FIGURE 3 shows the L_P (Fe-Mn-$C_{satd.}$) as a function of manganese content. The L_P values decrease with increasing manganese content in all cases. When plotted in FIG.4 as log f_P (Fe-Mn-$C_{satd.}$) vs. manganese content, all plots in FIG.3 are represented by a single straight line, regardless of slag composition and temperature. The slope gives -0.0029 for $e_P{}^{Mn}{}_{,C_{satd.}}$, independent of temperature, meaning that an addition of manganese to carbon saturated iron decreases the activity coefficient of phosphorus. When the solubility of carbon in Fe-Mn alloys, which was simultaneously determined and is shown in FIG.5, is extrapolated to unity for Mn/(Fe+Mn), the manganese content of an unstable Mn-C melt at 1573 K at carbon saturation is 92.7 mass pct, giving 0.53 for $f_P{}^{Mn}{}_{,C_{satd.}}$ for the Mn-C melt, where the standard state of phosphorus is that in carbon saturated iron. This indicates that phosphorus in carbon saturated manganese is more stable than in carbon saturated iron by -8.3 kJ/mol (= $8.314\times10^{-3}\times1573\times\ln 0.53$). Lee[3] estimated the standard Gibbs energy for Eqs.(3) and (5) as Eqs.(4) and (6), respectively.

$$P(l) = P(X)_{\text{in Mn}} \quad (3)$$

$$\Delta G^\circ = -203{,}611.4 + 41.003T \quad \text{(J/mol)} \quad (4)$$

$$P(l) = P(X)_{\text{in Fe}} \quad (5)$$

$$\Delta G^\circ = -159{,}499.3 + 19.891T \quad \text{(J/mol)} \quad (6)$$

Equations (4) and (6) give -139.1 and -128.1 kJ/mol at 1573 K, respectively. Equation (2) shows that phosphorus in carbon saturated iron is less stable by 19.4 kJ/mol than that in pure iron. Combining all those values, phosphorus in carbon saturated manganese is estimated less stable by 22.1 kJ/mol than that in pure manganese, leading to give $f_P{}^C$ (Mn-$C_{satd.}$)= 5.3, which is slightly larger than that for iron, 4.4, calculated from Eq.(2). The relationships of those values are schematically shown in FIG.6.

Using Eqs.(4) and (6), the values for ep^{Mn} for Fe-Mn melts may be evaluated according to Eqs.(7) and (8).

$$f_P^{Mn} = \frac{K_5}{K_3} \cdot \frac{M_{Mn}}{M_{Fe}} \quad (7)$$

$$\log f_P^{Mn} = e_P^{Mn}[\text{mass pct Mn}] \quad (8)$$

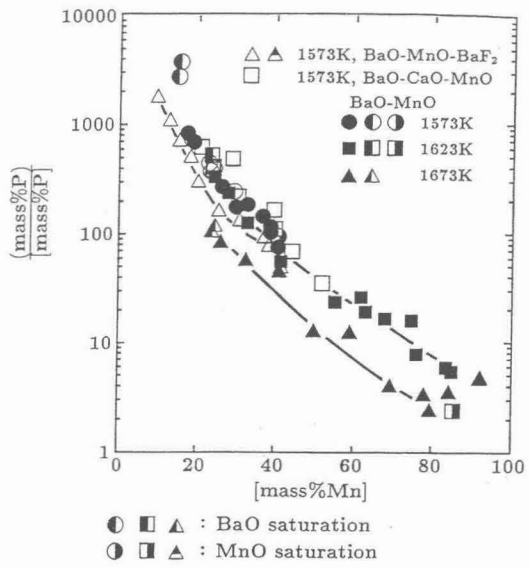

Fig. 1. Phosphorus partition ratio between BaO-MnO flux and Fe-Mn-$C_{satd.}$ alloy t 1573, 1623, and 1673 K as a function of Mn content of Fe-Mn-$C_{satd.}$ alloy.

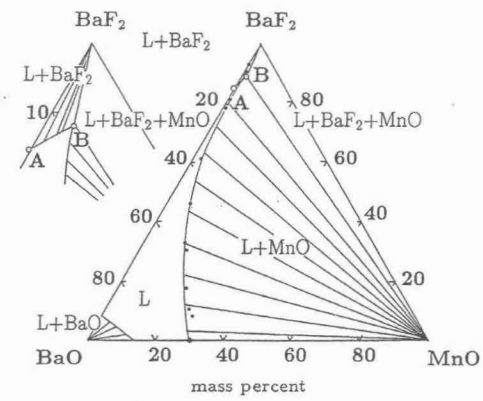

Fig. 2. Solubility of MnO in the BaO-BaF_2 system at 1573 K.

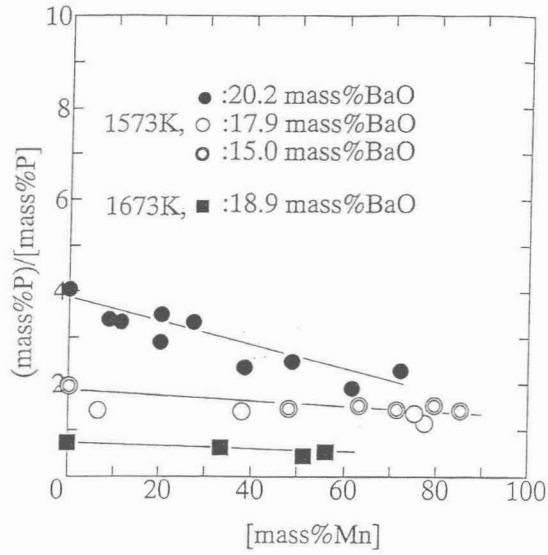

Fig. 3 Effect of manganese on the phosphorus partition between Fe-Mn-$C_{satd.}$ alloy and BaO-BaF_2 fluxes.

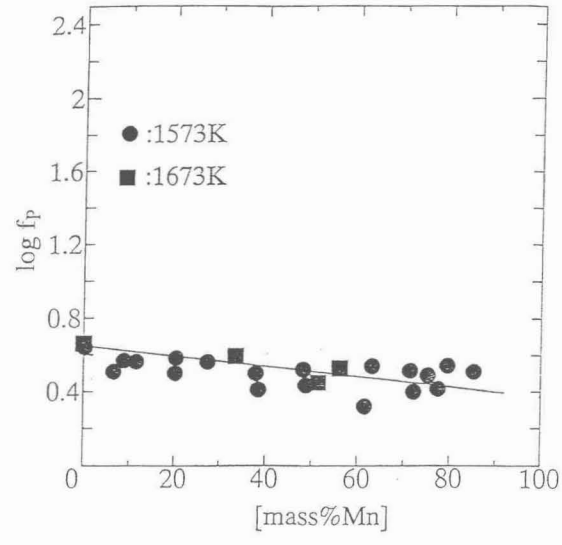

Fig. 4. Effect of manganese on the activity coefficient of phosphorus in Fe-Mn-$C_{satd.}$ melts.

where M denotes molecular weight. Equation (8) gives e_P^{Mn} as -0.0039 and -0.0027 at 1573 and 1673 K, respectively. They are in good agreement with the present value of -0.0029, which is valid only at carbon saturation. Schenck et al.[4] reported ε_P^{Mn} as 0 between 1788 and 1923 K, whereas Ban-ya et al.[5] showed $\varepsilon_P^{Mn} = -7.17$ or $e_P^{Mn} = -0.032$ up to 19.3 mass pct manganese at 1673 K. The present value is one order of magnitude smaller than the value of Ban-ya et al.

Liu[6] derived Eq.(9) for the activity coefficient of phosphorus in Mn-C alloys containing a small amount of phosphorus relative to pure liquid phosphorus, γ_P.

$$\ln \gamma_P = -10.64 + 14.27\, X_C + 30.6 X_C^2 \qquad (9)$$

Substituting $X_C = 0.257$ at carbon saturation at 1573 K into the last two terms in Eq.(9) yields 295 for f_P^C, which is far larger than 5.3 by the present estimation, probably because Eq.(9) might not hold at carbon saturation.

As mentioned earlier and seen in FIG.7, MnO contents of the fluxes are limited (the maximum content is 0.6 mass pct.), so that the effect of MnO on the activity of phosphorus in the flux may be ignored.

II. DETERMINATION OF THE ACTIVITY COEFFICIENT OF PHOSPHORUS IN CARBON SATURATED Mn-Si ALLOYS

When the alloy contains a large amount of silicon, the activity coefficient of phosphorus is known to be enhanced to have a relatively high partial pressure of phosphorus. For this reason, the partial pressure was controlled by equilibrating carbon saturated Fe-Mn-Si alloys with CaC_2, Ca_3P_2 and C at 3.33×10^{-4} atm of P_{P_2} at 1573K, according to Eqs. (10) and (11) as demonstrated in FIG.8.

$$3CaC_2(s) + P_2(g) = Ca_3P_2(s) + 6C(s) \qquad (10)$$

$$\Delta G^\circ = -383{,}160 + 177T \text{ (J/mol)} \quad [7),8)] \qquad (11)$$

Phosphorus in the alloy is equilibrated with P_2 according to Eq. (12)

$$1/2P_2(g) = P(X)_{\text{Mn-Si-Csatd.}} \qquad (12)$$

$$K_{12} = \frac{\gamma_P \cdot X_P}{P_{P_2}^{1/2}} \qquad (13)$$

$$\ln \gamma_P = \varepsilon_{P,Csatd.}^{P} \cdot X_P + \varepsilon_{P,Csatd.}^{Si} \cdot X_{Si} + \varepsilon_{P,Csatd.}^{Ca} \cdot X_{Ca} \qquad (14)$$

Rearranging Eqs.(13) and (14) yields Eq. (15).

$$\ln \frac{1}{X_P} - \varepsilon_{P,Csatd.}^{P} \cdot X_P - \varepsilon_{P,Csatd.}^{Ca} \cdot X_{Ca} + \frac{1}{2} \ln P_{P_2} = -\ln K_{12} + \varepsilon_{P,Csatd.}^{Si} \cdot X_{Si} \qquad (15)$$

If the left hand side, which is experimentally determined, is plotted against X_{Si}, ignoring the $\varepsilon_P^{Ca} X_{Ca}$ term because of a small content of calcium in the alloy and using $\varepsilon_P^P = 16.7$[3], a linear relationship with a slope of ε_P^{Si} and an intercept of $-\ln K_{12}$ will be obtained. FIGURE 9 shows the relationship between X_P and X_{Si} at constant $P_{P_2} = 3.33\times10^{-4}$ atm at

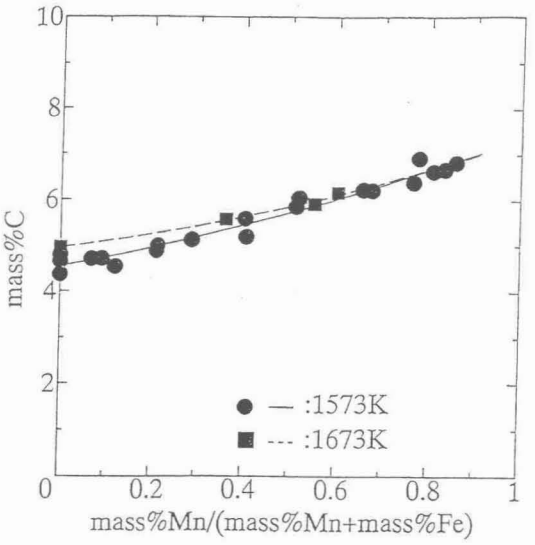

Fig. 5. Effect of manganese on the carbon solubility of the Fe-Mn-$C_{satd.}$ system

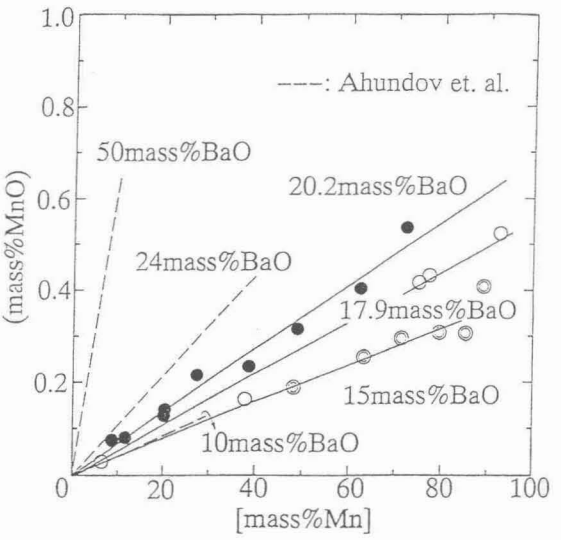

Fig.7. Relationship between manganese content of Fe-Mn-$C_{satd.}$ melts and $BaO-BaF_2$-MnO fluxes at 1573 K.

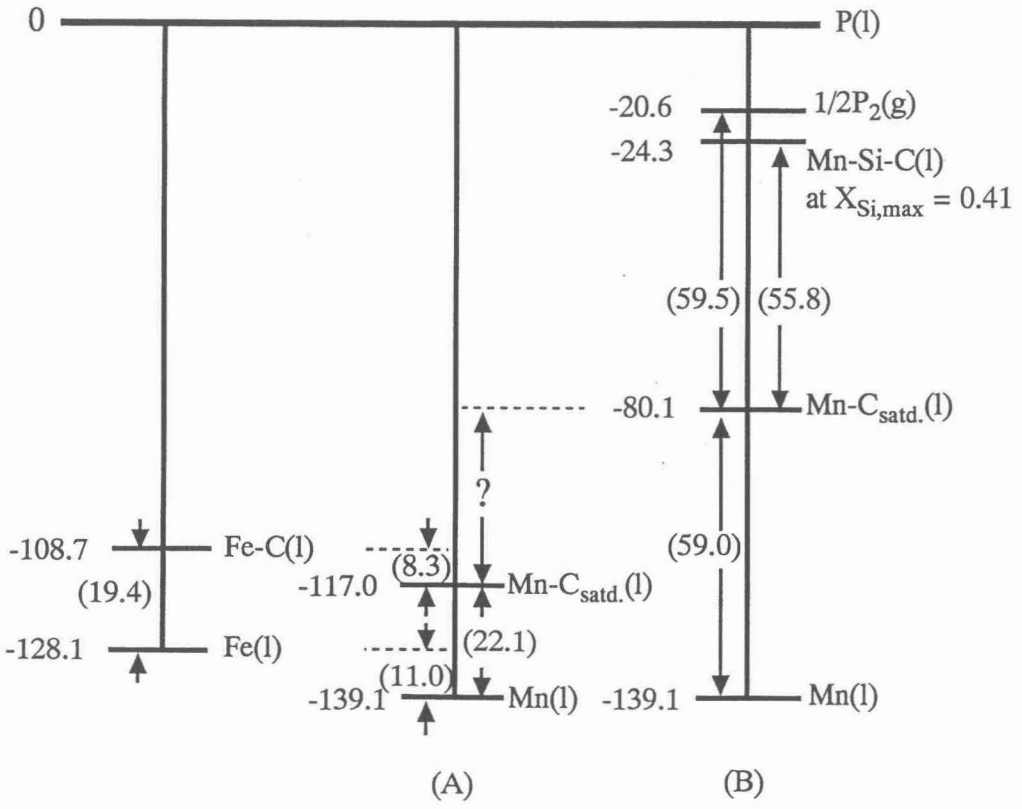

Fig.6 Estimated Gibbs energies of phosphorus in Fe-C and Mn-C melts relative to P(l) at 1573K. (kJ/mol) (A): from the experimental results in section A, (B): from those in section B.

1573 K and the same data (1/2 ln P_{P_2} (atm) = -4.0 was used in FIG.9) are plotted in FIG.10 according to Eq. (15), giving $\varepsilon_P^{Si,Csatd.}$ = 10.4 and ΔG°_{12} = -59.5 kJ/mol at 1573 K. Combining this value with -20.6 kJ/mol at 1573 K for Eq.(17), the Gibbs energy of phosphorus relative to P(l) is -80.1 kJ/mol, which means that phosphorus in carbon saturated manganese is less stable by 59.0 kJ/mol (this gives 91.0 as $f_P^{C,\ Csatd.}$) than in pure manganese.

$$P(l) = 1/2P_2(g) \qquad (16)$$

$$\Delta G^\circ = 62675.4 - 52.950T \quad (J/mol)\ ^{3)} \qquad (17)$$

This last value is much larger than 21.7 kJ/mol obtained in Section A. The reason for discrepancy is not clearly known but presumably due to employment of the value of e_P^P, which is valid only for a melt without carbon, and neglect of the $\varepsilon_P^{Ca}X_{Ca}$ term in Eq.(14). Another conceivable reason could be that because of a relative large concentration of phosphorus in Mn-Si-C alloys in the present case as seen in FIG.9, the activity coefficient of phosphorus may not be described only by the term of first order of X_P and a second order term may be needed. Accordingly, we are presently measuring the activity coefficient of phosphorus in a dilute concentration range by equilibrating the metal in a flowing argon with a fixed partial pressure of phosphorus together with molten silver as a reference.

III. DETERMINATION OF THE ACTIVITY OF MANGANESE AND CARBON IN A MOLTEN Mn-C MELT[9)]

The activity of manganese in a Mn-C melt in an Al_2O_3 or MgO crucible was determined by equilibrating it at 1628K with a solid MnO pellet in an Ar-CO mixture according to Eq.(18).

$$MnO(s) + C(s) = Mn(l) + CO(g) \qquad (18)$$

$$\Delta G^\circ = 286{,}800 - 170.2(\pm 2{,}500)T \quad (J/mol)\ ^{10)} \qquad (19)$$

$$K_{18} = \frac{a_{Mn} \cdot P_{CO}}{a_C} = \frac{\gamma_{Mn} \cdot X_{Mn} \cdot P_{CO}}{\gamma_C \cdot X_C} \qquad (20)$$

$$\ln \frac{P_{CO}(1 - X_C)}{X_C} = \ln K_{18} + \ln \frac{\gamma_C}{\gamma_{Mn}} \qquad (21)$$

where $\ln \gamma_C$ is described as Eq. (22).

$$\ln \gamma_C = \ln \gamma_C^\circ + \varepsilon_C^C X_C + \rho_C^{CC} X_C^2 + \rho_C^{CC} X_C^3 \qquad (22)$$

where γ_C° is the Raoultian activity coefficient of carbon at infinite dilution.
The Gibbs - Duhem relationship yields Eq. (23).

$$\ln \gamma_{Mn} = -\frac{1}{2}\varepsilon_C^C X_C^2 + \rho_C^{CC} X_C^3 \qquad (23)$$

At carbon saturation, Eq. (22) deduces

$$\ln \gamma_C^\circ = -\ln X_C^{satd.} - \varepsilon_C^C [X_C^{satd.} - \frac{1}{2}(X_C^{satd.})^2] + \frac{3}{2}\rho_C^{CC}[(X_C^{satd.})^2 - \frac{2}{3}(X_C^{satd.})^3] \qquad (24)$$

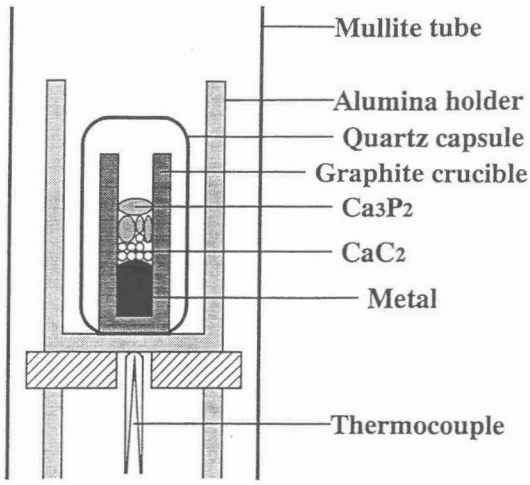

Fig. 8 Illustration of experiment arrangements for equilibration

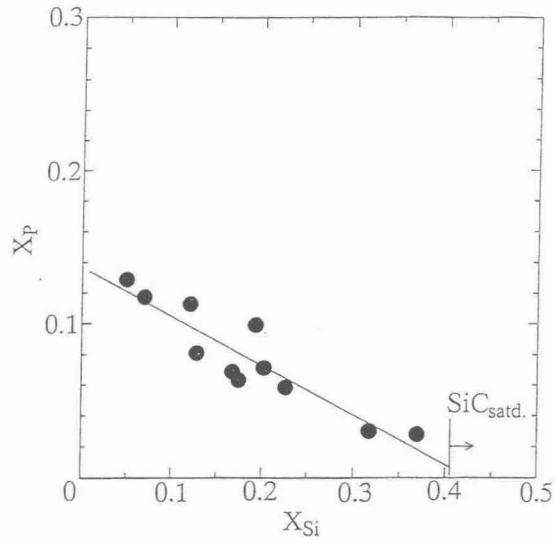

Fig. 9 Effect of silicon on the phosphorus content in Mn-Si-$C_{satd.}$ melts at 1573K.

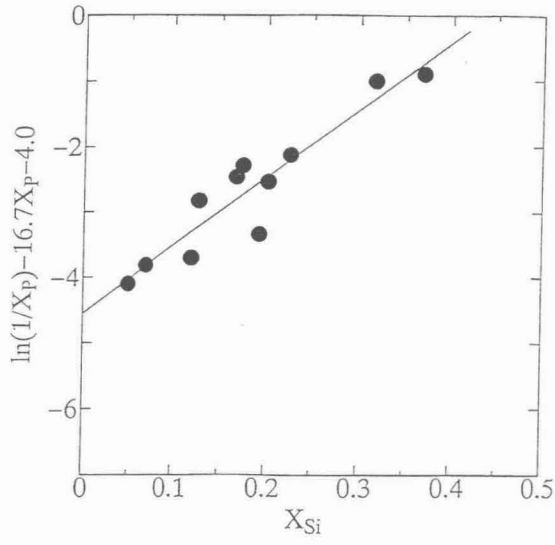

Fig. 10 Relationship between (ln(1/Xp)-16.7Xp-4.0) and silicon content in Mn-Si-$C_{satd.}$ melts at 1573K.

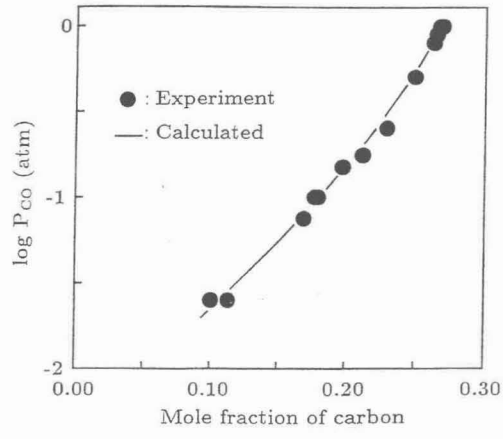

Fig. 11 Relationship between partial pressure of CO and carbon content of Mn-C alloy at 1628 K.

where $X_{Csatd.} = 0.268$ at 1628 K.
Substituting Eq.(24) into Eq. (21), Eq. (21) may be written as Eq. (25).

$$\ln\frac{P_{CO}(1-X_C)}{X_C} = \ln K_{18} - \ln X_C^{satd.} + \varepsilon_C^{C}[X_C - X_C^{satd.} + \frac{1}{2}(X_C^{satd.})^2] - \frac{3}{2}\rho_C^{CC}[X_C^2 - (X_C^{satd.})^2 + \frac{2}{3}(X_C^{satd.})^3] \quad (25)$$

By linear multiple regression analysis of the data plots according to Eq. (25), namely $\ln\frac{P_{CO}(1-X_C)}{X_C}$ vs. X_C, the following parameters were determined:

$\ln K_{18} = -0.879 (K_{18}=0.415)$, $\varepsilon_C^{C} = -10.9$, $\rho_C^{CC} = -46.8$, $\rho_C^{C} = 75.6$
and

$$\ln \gamma_{Mn} = 5.47X_C^2 - 46.8X_C^3 \quad (26)$$

$$\ln \gamma_C = -0.291 - 10.9X_C + 75.6X_C^2 - 46.8X_C^3 \quad (27)$$

The standard Gibbs energy for the reaction (18) calculated from ln K = -0.879 differs from Eq.(19) which gives ln K=0.718(K=0.488), only by 2.2 kJ/mol which is within the error of Eq. (19) This probes the accuracy of the present measurement.

FIGURE 11 shows the experimental and calculated relationship between log P_{CO} and X_C, the curve representing the data very well.

FIGURE 12 shows the activities of carbon and manganese in the Mn-C melt at 1628K, which are calculated using Eqs. (26) and (27), being compared with the results of other investigators.[10)-14)] At carbon saturation the activity of manganese negatively deviates from ideal behavior, being 0.40 at carbon saturation.

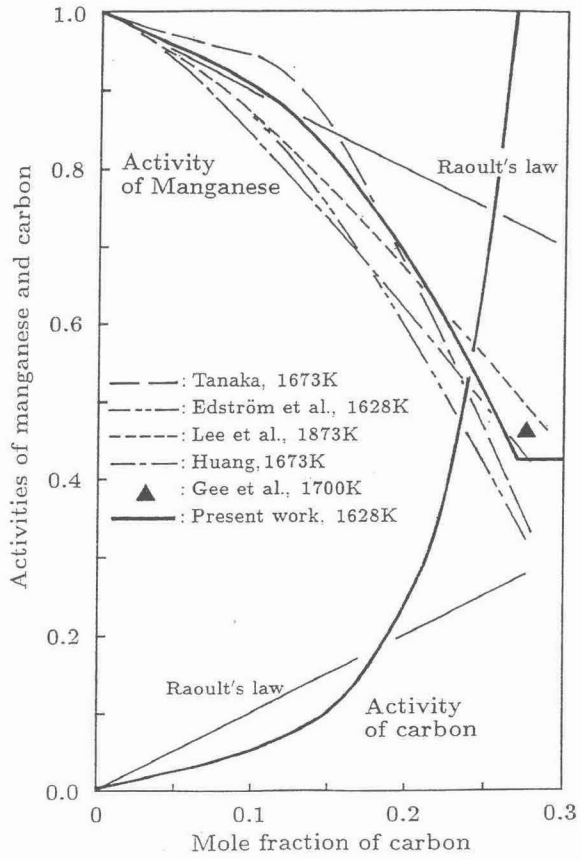

Fig. 12. The activities of manganese and carbon of liquid Mn-C alloys.

CONCLUSIONS

The thermodynamic properties of phosphorus in carbon saturated manganese and its ferrous alloys were investigated by using a chemical equilibration technique. The results are summarized as follows.

1. The activity coefficient of phosphorus is enhanced with adding manganese to carbon saturated iron with the interaction parameter of e_P^{Mn}, Csatd. being -0.0029 between 1573 and 1673K.
2. The activity coefficient of phosphorus in carbon saturated manganese is enhanced by the presence of carbon with f_P^C being equal to 5.
3. Silicon substantially enhances the activity coefficient of phosphorus with ε_P^{Si},Csatd. being equal to 10.4.
4. The activity of manganese deviates negatively from an ideal solution with being 0.40 at carbon saturation (X_C = 0.268) at 1628 K.

REFERENCES

1. Y.Watanabe, K.Kitamura, I.P.Rachev, F.Tsukihashi, and N.Sano, Metall.Trans. B, **24B**(1993), 338
2. F.Tsukihashi, M.Nakamura, T.Orimoto and N.Sano, Tetsu-to-Hagané, **76**(1990), 1664
3. Y.E.Lee, Metall.Trans.B, **17B**(1986), 777
4. H.Schenk, E.Steinmetz, and H.Gitizad, Arch. Eisenhüttenwes., **40**(1969), 597
5. S.Ban-ya, N.Maruyama, and Y.Kawase, Tetsu-to-Hagané, **70**(1984), 65
6. X.Liu, Dissertation, Department of Production Technology, The Royal Institute of Technology, Stockholm, (1993)
7. D.J.Min and N.Sano, Metall.Trans.B, **19B**(1988), 433
8. H.Ono, F.Tsukihashi, and N.Sano, Metall.Trans.B., **23B**(1992), 313
9 A.Katsnelson, F.Tsukihashi and N.Sano, ISIJ. Int., **33**(1993), 1045
10. E.T.Turkdogan, PhysicalChemistry of High Temperature Technology, Academic Press, New York, NY, (1980), 7
11. R.Gee and T.Rosenqvist, Scand.J.Metall., **5**(1976), 57
12. A.Tanaka, J.Jpn.Inst.Met., **41**(1977), 601
13. Y.E.Lee and J.H.Downing, Can.Metall.Q., **19**(1980), 315
14. W.Huang, Scand.J.Metall.,**19**(1990), 26
15. J.O.Edström and X.Liu, Dephosphorization of Ferromanganese Melts Part 1, Theoretical Considerations, China-Sweden Symp., Stockholm, Sweden, May, (1992), 15